IET Radar, Sonar & Navigation

Research Article

IET Journals
The Institution of Engineering and Technology

Along-track SAR interferometry using a single reflector antenna

ISSN 1751-8784
Received on 24th September 2014
Revised on 30th December 2014
Accepted on 1st February 2015
doi: 10.1049/iet-rsn.2014.0413
www.ietdl.org

Sebastian Bertl ✉, *Paco López Dekker, Marwan Younis, Gerhard Krieger*

German Aerospace Center (DLR), Microwaves and Radar Institute, Münchner Strasse 20, 82234 Wessling, Germany
✉ *E-mail: sebastian.bertl@dlr.de*

Abstract: A method to generate several phase centres on a single parabolic reflector antenna fed by a digital beamforming array is presented. Among other applications, along-track SAR interferometry at higher frequencies, as for example, in the Ka-band, is considered. Flexibility in size, position and amount of phase centres is similar as for a setup using a direct radiating array.

1 Introduction

Reflector antennas together with digital feeds for SAR applications have been studied intensively since several years [1]. This paper discusses the implementation of a multiple-phase-centre SAR system using a single reflector antenna in combination with a digital array of feed elements. Promising applications of this novel technique are along-track interferometry (ATI) and ground moving target indication (GMTI), although the same technique may find use for other purposes such as high-resolution wide-swath SAR imaging. ATI and GMTI are well-established techniques for satellite-based SAR systems, with applications in the field of road surveillance, land and maritime traffic monitoring or the measurement of ocean currents.

The formation of several phase centres on a reflector antenna by a controlled illumination of parts of the reflector has already been described in the open literature [2, 3]. Two ways of realisation have been proposed in [2], the feed pointing method, which aims at directing a single feed horn placed in the focal point of a reflector away from the centre of the reflector. The second method is based on the utilisation of a single multimode feed horn. The feed pointing method shows obvious shortcomings in realisation, as for example a mechanical rotation of feeds would be required as mentioned in [2]. In contrast, the described multimode feed horn antenna is operated with two waveguide modes (TE_{11} and TE_{21}) in order to generate two independent phase centres. The simultaneous use of several multimode feeds besides each other is not considered and would also cause problems regarding placement, since the associated far-field beams would point in different directions, as the feeds cannot all be placed in the focal point. The number of phase centres is described by the number of waveguide modes and is limited to two in the mentioned publications [2, 3]. Moreover, the size of the aperture illumination area corresponding to each phase centre is determined by the size of the feed horn and is not changed. To overcome these limitations, we suggest using a digital feed array that enables a highly flexible generation of multiple phase centres on the aperture area of the reflector.

To further illustrate the need for the flexible generation of multiple phase centres, a typical setup used for ATI with a direct radiating array (DRA) as shown schematically in Fig. 1*a* is considered.

The displaced phase centre antenna (DPCA) [4] condition for efficient clutter suppression is met if the pulse repetition frequency (PRF) is chosen such that the multiple displaced phase centres sample with subsequent pulses are at the same spatial positions. If planar direct radiating antennas are replaced by several reflector-based antennas, as in Fig. 1*b*, a lot of the flexibility is lost, as it will be explained in the following Section 2. This limitation can, however, be overcome by using a single reflector in combination with a digital feed array as described in detail in Section 3. In Section 4, simulations of the new reflector antenna technique are shown. Section 5 shows a system example, discusses possible applications of the presented method and explains the required steps regarding calibration before concluding the paper in Section 6 with final remarks.

2 Reflector antennas in ATI SAR applications

The considered reflector antennas have a parabolic curvature and in general an array of feed elements that is centred around the focal point of the reflector. The parabolic reflector could also be replaced by a reflectarray. The Rx signals of each feed are digitised and available for further processing. In the case of only one active feed element, the field strength (and surface currents) at the edge of the reflector is typically 8–10 dB lower than in the centre [5]. Compared with the sinc-like pattern of a rectangular antenna aperture with a uniform current distribution, the far-field beam pattern will be wider and can be expected to have lower sidelobes.

For the SAR system, the consequence of a wider beam is a larger Doppler bandwidth, and one option to avoid azimuth ambiguities would be to sample with a higher PRF compared with the case of a DRA. Placing several small reflectors with individual feed elements one beside the other as described before and shown on the right-hand side of Fig. 1 could theoretically fulfil the DPCA condition for a given PRF but will result in a SAR system with a very poor azimuth ambiguity level and will not allow a similar operation as in the case of a DRA with rectangular apertures. In addition, reducing the beamwidth by combining adjacent antenna elements is also not possible, because of the tapered surface currents that will generate a beam shape with additional amplitude modulations in the sidelobe region.

Overall, the direct implementation of an along-track SAR instrument by placing small reflectors in along-track direction besides each other will result in poor azimuth ambiguity suppression and is limited in terms of flexibility. The generation of several phase centres on a single reflector is an option to overcome this limitation.

3 Formation of phase centres on a reflector antenna using a digital feed array

A digital feed array can be used when multiple phase centres should be positioned on a single reflector antenna. In this context, the phase centre of an antenna is roughly defined as the virtual point, from

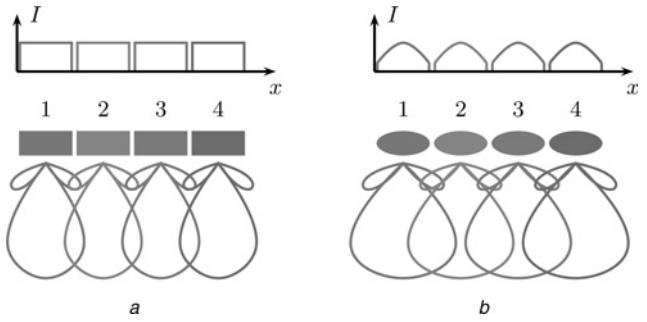

Fig. 1 *Schematic setup of two arrays consisting of planar antennas and reflector antennas*

Surface currents I on the single antennas are shown above and the far-field beams below the elements
a DPCA antenna
b Realisation with several small aligned reflectors

which the radiated fields can be imagined to emerge as spherical waves with ideal spherical wave fronts or equiphase surfaces [5]. This direct way of determining the phase centre is also applied in [2, 3] to determine phase centres for the case of a reflector antenna in combination with a multimode feed horn. A more specific definition depends on the antenna type and exists analytically only for very limited set of antennas. To the authors' knowledge, there exists no analytical solution for the calculation of the azimuthal position of the phase centre of a parabolic reflector when only parts of it are illuminated. Around each phase centre, a certain area of the reflector will reflect the incident electromagnetic field from the feed array to form the far-field pattern of the reflector antenna. This area of the reflector will be called aperture in the following, according to the direct relation of its physical dimension to the effective area or aperture for antenna types such as dish antennas [5].

In addition to the initially mentioned positioning capability, the amount of phase centres can be controlled and increased to considerably more than two depending on the amount of feed elements in the array. The size of the apertures corresponding to each phase centre can be adjusted as well. The probably most essential feature in terms of a later application is that the suggested concept can be implemented on any system that employs a large reflector antenna and a digital feed array for high-resolution wide-swath SAR imaging. Currently considered systems for future missions do therefore not need any hardware adaption in order to use the new multiple phase centre generation technique for interferometry as described in the following. This makes the described approach very appealing for current system studies. An existing airborne system that already shows all the required properties is the Ka-band SweepSAR system [6].

In the following, it is considered that the feed array is extended along the azimuth direction with several elements. The activation of a single feed element generates a narrow beam in a certain direction, as illustrated in Fig. 2*a*. Each feed will therefore acquire a different parts of the Doppler band.

Assuming that all feeds of the reflector are activated simultaneously, a narrow primary beam will be generated. This is illustrated in Fig. 2*b* by the dashed lines originating from the feed array and pointing towards the reflector. By calibrating the transmit and receive modules, the fields of the different feeds are in phase and constructively generate the incident field on the reflector surface. The larger azimuthal extension of the feed array compared with a single feed element will have the consequence that only a part of the reflector is getting illuminated. On the reflector, surface currents are generated with an intensity proportional to the incident field generated by the feeds. This can be described mathematically by the relation between the surface current density $\boldsymbol{J}$ and the incident magnetic field $\boldsymbol{H}(\boldsymbol{J} = 2 \cdot \boldsymbol{n} \times \boldsymbol{H})$. Fourier transform pairs provide the relation between the surface currents and the far-field pattern. Note that far-field beams with an aperture in the centre of the reflector or fed by feeds close to the focal point will have a more ideal shape than

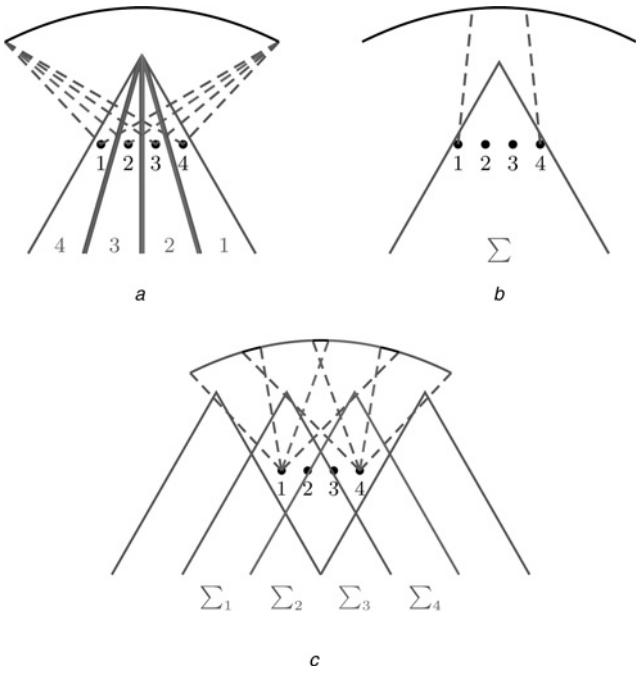

Fig. 2 *Illustration of beams resulting from different activation of azimuth feed elements*

a Activation of single feed elements
b Simultaneous activation of all feed elements in phase
c Simultaneous activation of all feed elements with linear phase offset between elements

beams originating from feeds further away from the focal point or with apertures on the sides of the reflector. In the considered applications, the focal distance F has to be large enough to avoid a strong beam degeneration in the considered angular intervals for the far field because of the effects of the reflector curvature and non-ideal focusing for feeds displaced from the focal point. According to basic Fourier correspondences, the smaller occupied area of surface currents on the reflector will lead to a wider beam.

For the case of ATI, mainly the azimuthal position of a phase centre is of interest. As an approach to approximate the azimuthal position of the phase centre x_{pc}, it is suggested here to determine the weighted centre of the surface currents J along azimuth on the reflector. However, a precise knowledge might have to be obtained by other means, for example, by measuring the phase of the far-field pattern, and optimising the flatness in the main lobe region and will be addressed briefly in Section 5.2.

By shifting the centre of the surface currents on the reflector, the phase centre can be shifted. Shifting of the surface currents is done by activating several feed elements to generate a narrow beam, that does not cover the complete reflector, and by additionally applying a phase term $\varphi(n)$ that changes linearly with the position of the feed elements according to

$$\phi(n) = \frac{2\pi}{\lambda} \cdot \Delta x_{\mathrm{feed}} \cdot \sin(\theta) \cdot n, \quad n = 0, \ldots, N-1 \qquad (1)$$

with Δx_{feed} being the spacing between the elements, θ the steering angle of the primary beam that generates the surface currents and n the index of the specific feed element. This concept, which is commonly applied to phased arrays, can be utilised in both the transmit and receive cases. The number of independent phase centres, that can be generated simultaneously to receive signals, is equal to the number of feed elements. The described concept is illustrated in Fig. 2*c*. Each far-field beam will be generated by surface currents that occupy only a narrow part on the reflector. The resulting beams will be wider than the beam of a single element. All beams will look in the same direction, but their phase centres are at different positions. With these properties, the beams

originating from a digital feed array and a single reflector can be used for ATI.

The resulting setup using a reflector antenna can be compared with the classical ATI configuration using a DRA. The number of independent phase centres is determined by the number of feed elements in the reflector case and by the number of array elements in the DRA case. The size of the apertures for each phase centre is determined by the size of the activated part of the feed array and consequently by the size of the reflector surface on which surface currents are being generated. The position of the phase centres can be set in a discrete way for the DRA in the case that specific parts of the array are activated. In the case of a reflector antenna, the phase centres can be shifted almost arbitrarily in position by modifying the phase of the feed signals. A higher flexibility in positioning the phase centres is given for the reflector-based case, since the shifting is done by multiplying phase terms on the signals of the feed elements and no amplitude changes are required, that would limit the applicability in the transmit case.

4 Example of reflector-based beamforming

An example of a reflector antenna with a feed array along azimuth, as it could also be used in a spaceborne SAR sensor, is analysed in the following. The consideration is based on a setup in Ka-band ($f = 35.5$ GHz).

An exemplary reflector antenna is modelled and simulated in the following using GRASP [7].

A reflector with an azimuth dimension of $L_a = 8$ m and a feed array centred around its middle is considered. The feed array consists of five elements, each with a dimension of 0.8λ, which results in an overall azimuthal dimension of the feed array of 4λ. A three-dimensional model of the setup simulated in GRASP is shown in Fig. 3. Parameters of feed and reflector are summarised in Table 1.

When all elements are activated, with equal phase on all feed elements, the surface currents are generated in the centre of the reflector. The resulting far-field pattern is centred around 0°. When surface currents should be excited on another part of the reflector, the signals of the different feed elements are generated on transmit or processed on receive with a linear phase offset with respect to each other according to (1).

Examples of surface currents that are not in the centre of the reflector are shown in Fig. 4. In these cases, the main beam is still directed towards 0° as shown in Fig. 5, whereas the phase centres, which approximately correspond to the centre of the surface currents, are in different regions of the reflector. For an SAR application this means that the shown beams illuminate the same region on ground, but from different phase centres as it is required for interferometric applications. Losses in gain and different beam shapes can be corrected during SAR processing from the known antenna pattern but are already below 2 dB in the far-field plots in Fig. 5.

5 Applications

5.1 ATI system example

ATI and GMTI have been demonstrated with airborne systems, and also with the dual receive antenna mode [8] of the space-borne systems RADARSAT-2 and TerraSAR-X. In a two-channel ATI configuration, the Doppler information is derived from the phase of the interferogram formed by combining the pair of focused SAR images corresponding to the two phase centres. Two-channel ATI performs, however, poor for GMTI applications, where the static clutter signal level may often exceed that of the moving target. Clutter suppression can be achieved in a two-channel system using the DPCA condition, where the difference of the two SAR images is generated, hereby suppressing the clutter, which is common for both. Although DPCA originally was developed for dual-channel systems, it also can be used with more than two channels [9]. Different requirements on swath width and occurring velocities of the moving objects can lead to different ideal sizes of the single antennas for each channel.

Table 1 Parameters of feed and reflector in the considered example

Parameter	Value
reflector: width, height	8 m, 1.2 m
focal length F	8 m
single feed: width, height	0.8 λ, 14 λ
azimuth element spacing	0.8 λ
number of feeds along azimuth	5
clearance	0 m

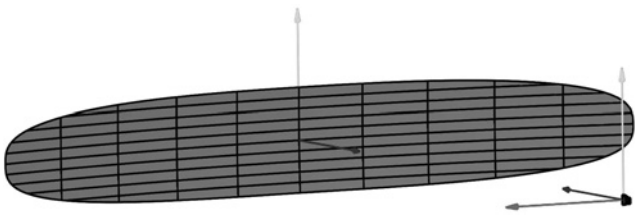

Fig. 3 *Three-dimensional model of the reflector antenna and the feed array simulated with GRASP [7]*

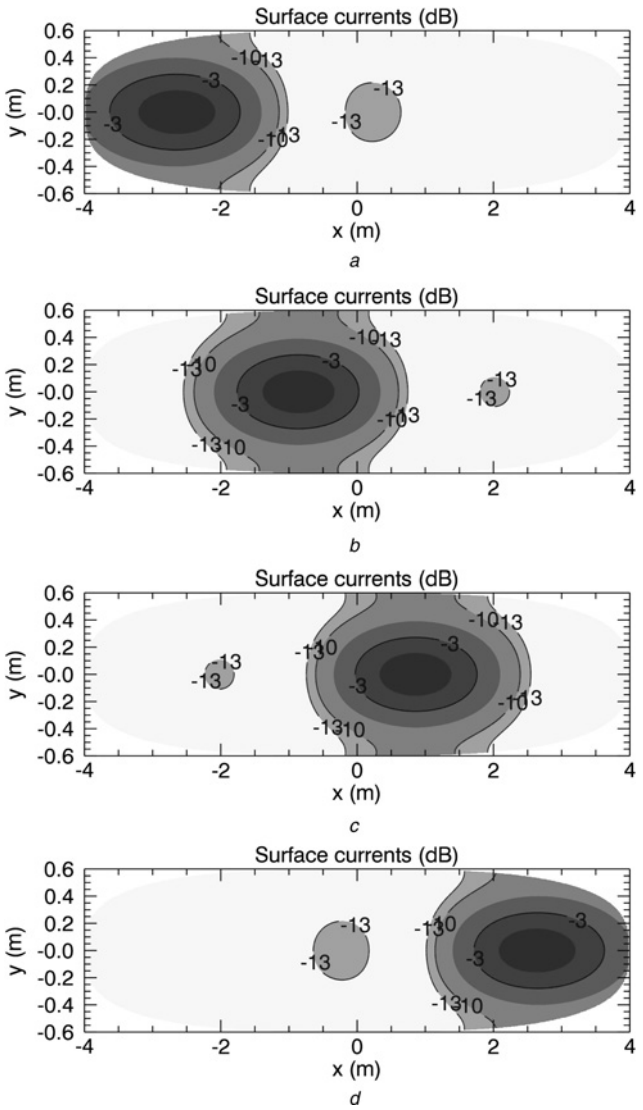

Fig. 4 *Surface currents on the parabolic reflector for different phase shifts applied to the feed array elements according to (1)*

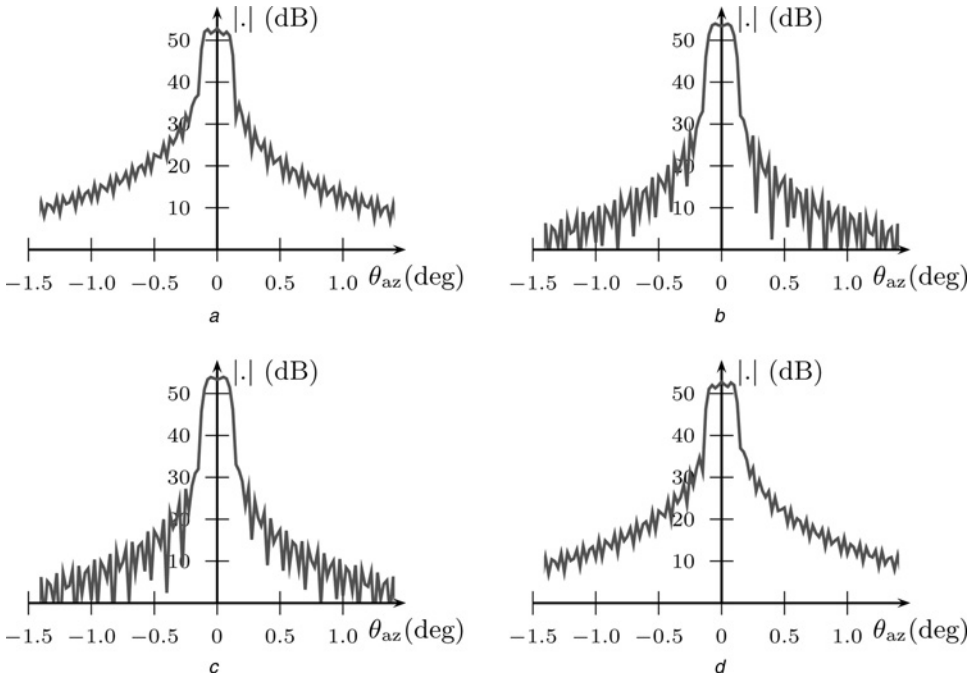

Fig. 5 *Far-field plots generated from surface currents as shown in Fig. 4*

The implementation of ATI with a single reflector antenna is especially interesting at higher frequencies, for example, Ka-band, since the required along-track baselines for applications like the measurement of ocean currents or land traffic monitoring, are in the order of few metres or below and could be implemented efficiently on a single platform [10]. At Ka-band, system studies show that losses in transmission lines and switching networks are high. The design of an efficient system using DRAs is difficult, when baselines of several metres should be generated. The benefit of a reflector-based antenna setup would be that it keeps the feed array and its radio-frequency network compact and close to the satellite body as it would be desirable in terms of low system losses. Planned missions using Ka-band frequencies as the surface water and ocean topography (SWOT) mission [11] and current studies [12] are based on structures that span physical baselines of 10–20 m. In the case of the SWOT mission, a reflectarray with 5 m length is used. Similar antenna dimensions are of interest for ATI in the current context.

A possible schematic antenna setup that exploits the concept of ATI using a single reflector antenna is shown in Fig. 6. The schematic setup shows one large reflector that is illuminated by a feed array placed in the focal point of the reflector. The system can be operated in different configurations, in order to adapt amount and size of the phase centres to different scenarios. The setup can be changed electronically during flight depending on the desired application.

Both size and position of the phase centres and corresponding apertures can be modified. As an example, two modes are shown in Fig. 6. The first mode, with smaller apertures for each phase centre but higher number of phase centres, will result in higher resolved images with very good clutter suppression because of the availability of several displaced phase centres. It could therefore be used for GMTI above land. For the measurement of ocean currents, resolution requirements are typically lower and the SAR system could be operated with larger apertures, less phase centres and therefore lower PRF and larger swath as shown in Fig. 6*b*.

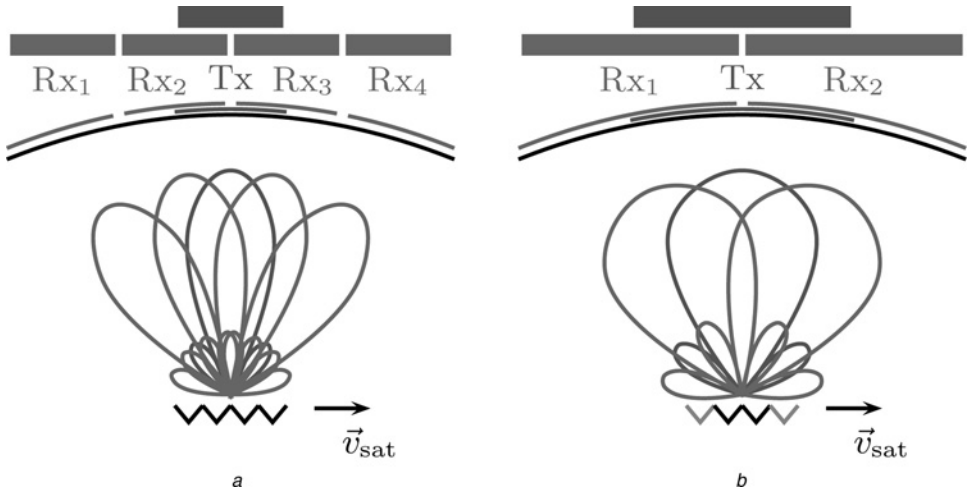

Fig. 6 *Schematic illustration of a setup with a single reflector antenna that can be used for ATI-SAR in different modes regarding size, position and amount of phase centres and therefore receive channels*

a Four smaller Rx phase centres (lower line) and one Tx phase centre, with wider far-field beams
b Two phase centres on receive, one on transmit (only two feeds active)

For a simulation of the SAR performance, the example shown in Figs. 4 and 5 is picked up, since it also consists of four phase centres. To show that the four phase centres show similar performance among each other in a SAR application, the azimuth ambiguity to signal ratio (AASR) is calculated. The PRF is set to 7 kHz. The Doppler band and the four closest ambiguity bands for a phase centre at the edge and a phase centre in the centre of the reflector antenna are shown in Figs. 7*a* and *b*. The AASR value for all four phase centres at a look angle of 31° is plotted in Fig. 7*c*. The values are similar for all the four phase centres, differing by only 2 dB. The four phase centres can therefore be used with the proposed PRF in an along-track configuration without a large difference in performance between them. Larger differences in the performance would require higher PRF values for a sufficient performance of only few phase centres but with a loss in other system parameters such as swatch width. Along range, the ambiguity suppression will mainly depend on the number of feed elements that are available for digital beamforming (SCan-On-REceive, SCORE) and the antenna height. The performance along range can therefore be optimised independently from the azimuth performance equivalent to the case of a SAR system with a reflector antenna with only one azimuth channel and is therefore not specifically discussed.

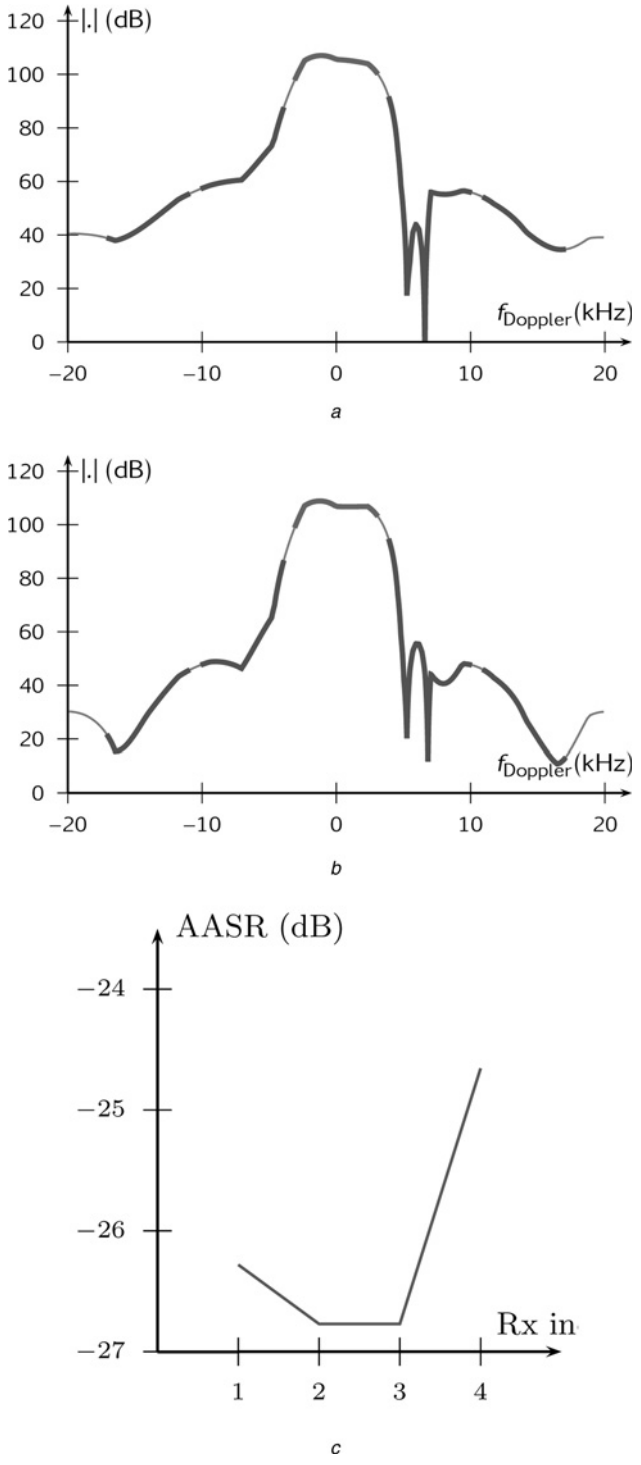

Fig. 7 *Azimuth performance of the four Rx channels (PRF = 7 kHz, look angle 31°)*

a Signal and ambiguity Doppler bands for Rx 1
b Signal and ambiguity Doppler bands for Rx 2
c AASR at 31° look angle

5.2 Calibration aspects

Owing to the small wavelength of 8.4 mm in case of a Ka-band system, the mechanical and thermal stabilities need to be addressed, especially when structures spanning several metres are required. For architectures with large booms of up to 10 m as in [12], metrological instruments placed close to the feed array are considered to measure the effect of oscillations of the boom and thermal distortions leading to geometrical deformation of them and resulting in a misplacement of the reflectors that are placed on the tip of the boom in this constellation. Especially, after manoeuvres to change the attitude of the satellite, the movements of the structure need to settle before new acquisitions. This needs to be considered in the operation of the system. In a similar way as effects of boom oscillations are measured above, the movement of different parts of one large reflector antenna could be monitored in the case considered here.

Regarding the interferometric baseline, a characterisation of the antenna on ground for different supplied phase terms as in (1) on the digital feed array can provide a first calibration. The location of the phase centres can be determined by the location of the surface currents on the reflector in this example. However, owing to the mentioned thermal and mechanical distortions, possible baseline variations need to be addressed in addition during flight. For a calibration during flight, the coregistration of the images to the different phase centres of a fixed target above land can provide a way to constantly calibrate the along-track baseline. Another approach is demonstrated in Fig. 8. The phase difference of the far fields of different phase centres is evaluated. Owing to the different phase centre positions, a phase difference in the far-field patterns over the look angle occurs. In the main lobe region for small angles θ_{az}, this phase change is almost linear and is related to the separation B of the phase centres, analogue to the case of

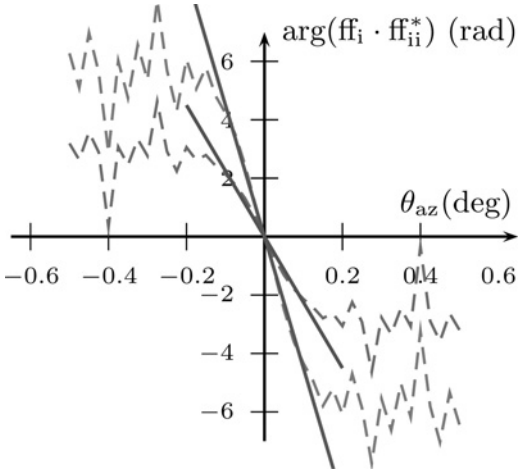

Fig. 8 *Phase difference of two pairs of far-field pattern of the four generated phase centres as in Fig. 4, smaller slope: middle two (Rx_2 and Rx_3 in Fig. 6a) and larger slope: middle and outer phase centre (Rx_2 and Rx_4 in Fig. 6a)*

IET Radar Sonar Navig., 2015, Vol. 9, Iss. 8, pp. 942–947

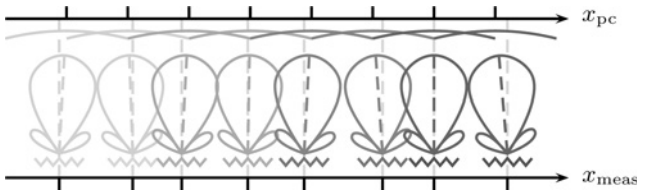

Fig. 9 *Placement of regularly spaced phase centres x_{pc} on a reflector antenna originating from irregular measurement positions x_{meas} as they result from a SAR system measuring with a variable PRF (staggered SAR)*

broadside arrays [5], through

$$B = \frac{\lambda}{2\pi} \cdot \frac{\Delta\Phi}{\Delta\theta_{\text{az}}} \tag{2}$$

where $\Delta\Phi$ is the phase change along the angular interval $\Delta\theta_{\text{az}}$ and λ is the wavelength.

Evaluating the linear slope in Fig. 8 results in distances between different phase centres. Two distances can be derived, one from an inner phase centre to the other inner phase centre (Figs. 4*b* and *c*) as $B_{\text{centre, centre}} = 1.70$ m and the other from an inner phase centre to an outer one (Figs. 4*b* and *d*) with $B_{\text{centre, side}} = 3.41$ m. These two relative distances correspond to positions of the phase centres along azimuth at the positions $x_{\text{az}} = \pm 0.85$ m, ± 2.56 m, such that according to Fig. 6*a* the positions of the phase centres would be $x_{\text{Rx}_1} = -2.56$ m, $x_{\text{Rx}_2} = -0.85$ m, $x_{\text{Rx}_3} = 0.85$ m and $x_{\text{Rx}_4} = 2.56$ m. These positions calculated using the linear slope in Fig. 8 also resemble the positions of the maximum surface currents in the four plots in Fig. 4.

5.3 Other applications

Applications in other areas than ATI can also benefit from the described technique. For the case of a changing PRF (staggered) SAR [13], the possible performance loss from non-uniform sampling could be avoided by shifting the phase centre on the reflector to the required position from pulse to pulse. The position of the virtual phase centre of a combination of Tx and Rx phase centres can be placed on receive channel, since the virtual phase centre lies in the middle of them. Since the receive channels are sampled digitally, this means that the effective phase centre can be selected independently for each transmit pulse and range after reception of the scattered signals in a processing step before the SAR focusing.

The reflector in this case needs to be large enough to be able to compensate the deviation of the actual satellite position ($\tilde{v}_{\text{sat}} \cdot \sum_m \text{PRI}_m$) with the used sequence of variable PRIs that can lie in the interval [PRI_{min}, PRI_{max}] to the desired position of the phase centres that lie at equally spaced positions $\sim v_{\text{sat}} \cdot m \cdot \text{PRI}_{\text{avg}}$. For this application, the positions of the phase centres need to be changed from pulse to pulse. The shift of the phase centre of a measurement in order to obtain equally spaced data samples is illustrated in Fig. 9.

6 Conclusions

A method to gain flexibility in number, position and size of phase centres for a reflector-based SAR system has been established. Owing to the availability of digitally sampled output for every receiver in the case of a digital beamforming SAR system, the adjustment of these parameters can be done during flight on a pulse-to-pulse basis. For the implementation of along-track SAR interferometry, it is possible to generate several phase centres on a common reflector in along-track direction. Since requirements change for different applications of ATI, as the monitoring of road traffic or the measurement of ocean currents, the flexibility of this approach allows one to easily adapt the system to different operational modes. Applications of interferometry at higher frequencies, for example, at Ka-band are of special interest, since the required baselines can fit on a single reflector antenna but also traffic monitoring at lower frequencies can be considered. Mapping unequally spaced measurement positions to equally spaced azimuth positions of the corresponding data samples can be useful when the PRF should be modified as in the staggered SAR concept.

In general, the same flexibility in size and amount of phase centres as for a DRA setup is possible using a single reflector with a feed array. The placement of the phase centres can be even done on transmit and receive channels in a precise way, since the placement depends only on the phase offset of the different feed elements and is not limited to discrete element positions of an array.

7 References

1 Krieger, G., Gebert, N., Younis, M., Bordoni, F., Patyuchenko, A., Moreira, A.: 'Advanced concepts for ultra-wide-swath SAR imaging'. Seventh European Conf. on Synthetic Aperture Radar (EUSAR) 2008, 2008, pp. 1–4

2 Damini, A., Balaji, B., Shafai, L., Haslam, G.: 'Novel multiple phase centre reflector antenna for GMTI radar', *IEE Proc., Microw. Antennas Propag.* , 2004, **151**, (3), pp. 199–204

3 Pour, Z., Shafai, L.: 'Investigation of virtual array antennas with adaptive element locations and polarization using parabolic reflector antennas', *IEEE Trans. Antennas Propag.*, 2013, **61**, (2), pp. 688–699

4 Dickey, F., Santa, M.: 'Final report on anti-clutter techniques'. Technical Report, Report R65EMH37, General Electric Co., 1953

5 Balanis, C.: 'Antenna theory, analysis and design' (Harper and Row, New York, 1982)

6 Sadowy, G.A., Ghaemi, H., Hensley, S.C.: 'First results from an airborne ka-band SAR using SweepSAR and digital beamforming'. Ninth European Conf. on Synthetic Aperture Radar, 2012, EUSAR, April 2012, pp. 3–6

7 TICRA: 'Grasp – Homepage', http://www.ticra.com/products/software/grasp, 2013 (Status: 8 July 2013)

8 Romeiser, R., Suchandt, S., Runge, H., Steinbrecher, U., Grunler, S.: 'First analysis of TerraSAR-x along-track InSAR-derived current fields', *IEEE Trans. Geosci. Remote Sens.*, 2010, **48**, (2), pp. 820–829

9 Lombardo, P., Colone, F., Pastina, D.: 'Monitoring and surveillance potentialities obtained by splitting the antenna of the COSMO-SkyMed SAR into multiple sub-apertures', *IEE Proc., Radar Sonar Navig*, 2006, **153**, (2), pp. 104–116

10 Bertl, S., López-Dekker, P., Baumgartner, S., *et al.*: 'Ka-band multi-baseline ATI-SAR system for ocean surface currents measurements'. First KEO Workshop (Ka-band Earth Observation Radar Missions), ESA, November 2012, pp. 1–8. Available at http://elib.dlr.de/79370/

11 Dibarboure, G., Labroue, S., Ablain, M., *et al.*: 'Empirical cross-calibration of coherent SWOT errors using external references and the altimetry constellation', *IEEE Trans. Geosci. Remote Sens.*, 2012, **50**, (6), pp. 2325–2344

12 Schaefer, C., Völker, M., Lopez-Dekker, P., Younis, M., Daganzo-Eusebio, E., Ludwig, M.: 'Space-borne ka-band across-track SAR interferometer'. Proc. First KEO Workshop, Noordwijk, The Netherlands, 2012, pp. 1–8

13 Villano, M., Krieger, G., Moreira, A.: 'Staggered SAR: high-resolution wide-swath imaging by continuous PRI variation', *IEEE Trans. Geosci. Remote Sens.*, 2014, **52**, (7), pp. 4462–4479